JOURNAL OF OPTOELECTRONICS AND ADVANCED MATERIALS Vol. 19, No. 1 - 2, January – February 2017, p. 66 - 72

Optical and microstructure characterisation of ceramic – hydroxyapatite coating fabricated by laser cladding

A. PASCU[a*], E. M. STANCIU[a], D. SAVASTRU[b], V. GEANTA[c], C. CROITORU[a]
[a]*Transilvania University of Brasov, 29 Eroilor Blvd., 500036, Brasov, Romania*
[b] *National R&D Institute for Optoelectronics – INOE 2000, 409 Atomistilor St, RO-077125 Măgurele Ilfov, Romania*
[c]*University POLITEHNICA Bucharest, 313 Splaiul Independentei, Bucharest 060042, Romania*

In this paper, a new approach in designing IR-absorptive Al_2O_3/TiO_2 glass/ceramic coatings through a one-step process involving laser cladding and by using hydroxyapatite as glass and hard phase ceramic former has been described and the optical and microstructural features of the material have been emphasised. To improve the bonding of the coating to the substrate, aluminium has been added in the ceramic starter paste composition. The coated layer is formed by crystalline Ir-absorptive ceramic phases entrapped in a dominatingly amorphous glassy matrix, at the interface with the copper substrate and by a predominant glassy structure, in the upper part of the coating. The results show good absorbance of the 35 μm-thick layer in the IR domain and good transparency in the 500-800 nm domain, reflecting the wavelengths corresponding to the copper substrate, coupled with a good-crack resistance and hardness, making our approach useful in designing colored solar absorbers.

(Received November 29, 2016; accepted February 10, 2017)

Keywords: Solar collectors, Reflectance, Laser cladding, Glass-ceramic phases, XRD spectroscopy

1. Introduction

Efficiency of the solar-thermal conversion systems mainly depends on the optical properties and thermal stability of the spectral-selective materials used as solar radiation absorbers. An efficient solar-absorptive layer is defined as having high absorptance values (in ideal cases the solar absorptance coefficient α_s= 1 in the 0.3-2.5 μm spectral range).

Among the spectrally-selective surfaces such as semiconductor-metal tandems, multilayer absorbers, ceramic-metal composite coatings (cermet) and textured surfaces, the ceramic-based ones are the most promising in terms of performance, versatile and well-studied.

Even though several high performance solar absorptive surfaces already exist on the market, they are still economically inefficient due to the high cost of the precursors and of the obtaining method.

To design materials for a sustainable development of the society, new efficient and environmentally friendly methods must be developed.

During the last decade, the laser cladding process has become a common technique to fabricate coatings on various types of substrates. The cladded layer is realized by using the laser beam as heating source and wire or powder as filler material [1]. There are three main methods used to perform the laser cladding which differ especially through the shape of the filler material and the ways in which it can be cladded: by wire feeding, by powder injection or with pre-placed powder [2].

Using wire or powders have advantages and disadvantages but adding or varying the alloy chemistry is an easy task in case of powders. The powder can be either injected coaxially with the laser cladding head or can be preplaced on the substrate and melted by the laser beam as a two-stage cladding technique. The preplaced technique is realized by mixing the powder with a chemical binder and placed in the form of paste on the base material.

HA combined with other ceramics materials can be used in a narrower field of application e.g. solar applications due to the specific optical proprieties, respectively the good IR absorbance and reflective of the visible light. Currently there are various methods to obtain ceramic coatings on nonferrous substrate, e.g. pulsed laser deposition [3, 4], plasma spraying [5], sol-gel [6, 7], electrochemical deposition [6-8], but a simple method to rapidly evaluate the potential of the coating is by preplaced laser cladding [9]. Huang at al. [10] synthesized hydroxyapatite coating by preplaced laser cladding using sodium silicate as adhesive for the powder mixture and obtained compact HA bio-ceramic coatings on commercially pure titanium grade Ta2 substrate. Different binders [11] like water glass or poly (vinyl alcohol) are tested for inter-particle adhesion improvement as well as in improving the bonding between coating and the substrate. Further improvement of the HA coatings can be obtained by the addition of carbon nanotubes that increases the microhardness of functionally graded bio ceramic-layer by 46.8% and almost double the bonding strength (28.2 MPa) compared with pure HA coating [12]. Mixing of HA with other ceramic oxide can increase the low mechanical proprieties of calcium phosphate which is inherently brittle. The aluminium and titanium oxide, in the form of dried powder or as preplaced paste, are commonly used for obtaining high quality ceramic coatings. Chen et al. [13] used spray-dried sintered Al_2O_3-13wt. %TiO_2 to obtain crack-free coatings with fine metallurgical bonding to the substrate. The same ceramic alloy is used [14] for laser cladding with induction heating to ensure a constant heating during the cladding process. Through this method temperature beyond 2045 °C was obtained as the aluminium oxide fully melted.

In this paper, a solar-absorptive coating has been obtained on copper substrate through laser cladding, starting from a mixture of aluminium and titanium oxides, with metallic aluminium added in composition to improve the adhesion of the coating to the substrate and hydroxyapatite (HA) as IR-absorptive ceramic and glass former.

2. Experimental procedure

2.1. Materials

The materials used for the ceramic coating obtaining are Metco® 131VF powder comprising of aluminium oxide in mixture with titanium oxide Al_2O_3+TiO_2, (Oerlicon Metco, USA), pure aluminium powder Al (Sigma-Aldrich, USA) and hydroxyapatite $Ca_{10}(PO_4)_6(OH)_2$ (Sigma-Aldrich, USA). All the reagents used were of analytical purity.

Rectangular electrolytic copper (99.99 % purity) plates with dimensions of 30x80x3 mm were used as coating substrate for the experiments. The Cu plates were cleaned by grinding on a P 600 grit paper and have been degreased in ethanol prior to use. The PVA binder decomposes at ~ 400 °C and is expected that during the coating fabrication, typical temperature of 1000-1500 °C are achieved and therefore no organic phase remains.

2.2. Methods

2.2.1. Coating fabrication

The laser cladding process of the glass/ceramic coating on copper consisted in two successive steps, namely pre-placement of the ceramic starter and laser melting of the powder mixture, described in the following paragraphs.

2.2.1.1. Pre-placement of the ceramic starter paste

The ceramic starter mixture has been obtained as a thick paste through mixing of the ceramic/metal powders with an aqueous solution of poly (vinyl alcohol). The mass ratio of the powders used in this study was 50% wt Metco® 131 VF, 25%Al and 25%HA. The mass ratio between the powder mixture and the organic PVA binder has been kept at 3:1. The obtained paste has been applied on the surface of the copper plates by using the Dr. Blade [15] technique, in an approximate thickness of 0.5 mm. The coated specimens were dried on a heating plate for 30 min. to evaporate the excess solvent and to form a continuous polymeric film, binding the particles together.

2.2.1.2. Laser melting

Laser cladding was carried out using a Coherent F1000 diode laser together with a Precitec WC 50 welding head manipulated by a CLOOS welding robot, Argon was used as shielding atmosphere surrounding the preplaced powder. Tilting of the cladding head at 3º in the cladding direction and defocused laser beam of 2 mm was used for the cladding tests. The standoff distance between the welding head and the substrate was set at 12.5mm.

12 partially overlapped tracks were realised on the sample with a scanning speed of 8mm/s and a laser power of 680W. Three identical samples were fabricated to validate the tests.

2.2.2. Analysis methods

After laser cladding etch sample was precision cut and prepared form microstructure investigation by grinding polishing and etching with a metallographic reagent representing a weight ratio mixture of $FeCl_3$: CrO_3: HCl 37%: distilled water = 5:1:1:20.

The microstructure of the coatings has been analysed through optical microscopy using an optical Olympus GX51 microscope and through electron micrographs, obtained by a scanning electron microscope (SEM) including and EDX (Quanta FEG 250, equipped with EDAX analyzer – FEI).

The structure and composition of the coating have been studied using an X-ray diffractometer (Bruker-AXS-D8) with CuKα radiation, in the range 2θ =10–70°. The crystalline and amorphous contributions have been quantified by spectral deconvolution of the diffractogram, by using Gaussian-Lorentzian profiles.

The VIS and NIR spectra have been acquired by using a Perkin-Elmer Lambda 90 spectrometer equipped with an integrating sphere, working in reflectance mode. The spectral resolution of the instrument has been set at 1nm.

The microhardness of the coatings was measured using a Shimadzu HMV 2T microhardness tester. Five $HV_{0.05}$ indentations on each zone with the following set-up: load 490 mN and dwell time of 10 sec.

3. Results and discussion

The photographic image of the copper plate with the pre-placed glass-ceramic starter powder used in this study and the glassy coating obtained through laser cladding is illustrated in Fig. 1a. It can be clearly observed from Fig 1. (a) that the addition of poly (vinyl alcohol) aqueous solution as binder in the composition of the powder mixture contributes to the obtaining of a ceramic-starter paste with high surface energy, which contributes to a uniform spreading on the copper substrate and improves the homogeneity of the mixture, by impeding the gravimetric separation of the particles. The overall dimension of the powders used in the starter-paste composition is 1-3 µm, with the hydroxyapatite particles having a higher average diameter (3-6 µm). The uniformity of the pre-placed ceramic coating starter could be also evidenced by the EDX elemental composition depicted from the surface of the coating (Fig. 2), which comprises all the main elements (Al, Ti, O, Ca, P) in an approximate ratio similar with the gravimetric fractions of the components in the prepared powder mixture receipt.

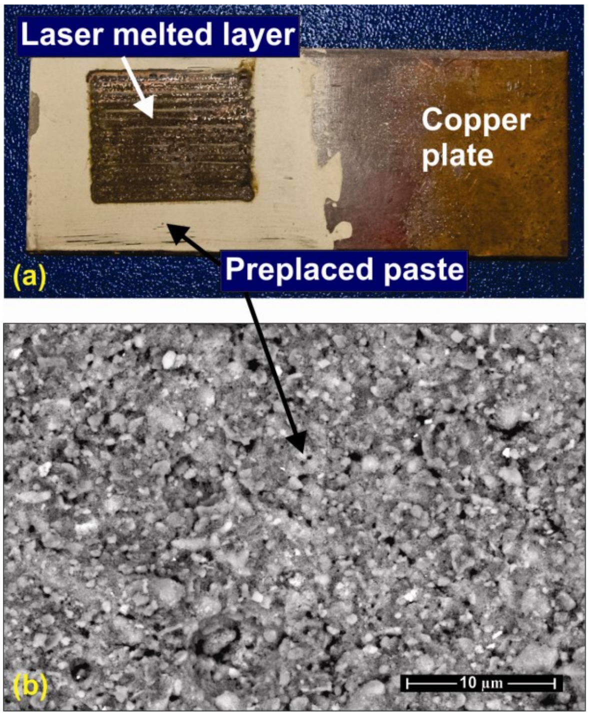

Fig. 1. a) Sample appearance after the laser melting, b) the SEM images of the preplaced powder before laser processing

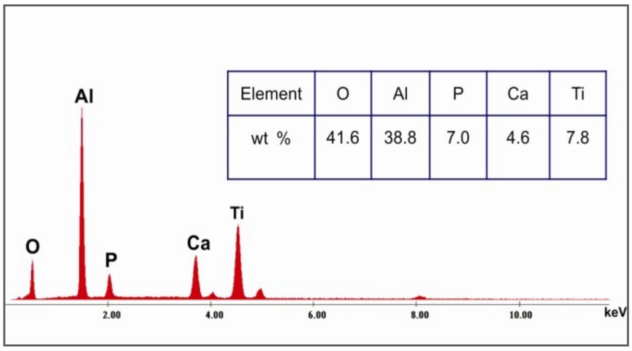

Element	O	Al	P	Ca	Ti
wt %	41.6	38.8	7.0	4.6	7.8

Fig. 2. EDX analyses of the pre-placed powder before the laser processing (EDS set-up: kV: 30.00 Tilt: 0.00 Take-off: 2.92 AmpT: 12.80)

Optical microscopy of the samples shows that a 15 to 40 µm glassy-ceramic layer was coated on the surface of the cooper substrate. The coated layer is not uniformly deposited on the copper surface and presents no visible transition line between the materials.

Fig. 3.a illustrates the geometrical appearance of the layer and the heat affected zone. The copper substrate presents visible heat affected zone (Fig. 3b) where a dynamic recrystallization up to 300 µm from the surface occurs due to the intense thermal gradient induced by the laser radiation (Fig. 3b). The recrystallization phenomena lead to the substrate hardness increasing from 63 $HV_{0.05}$ to 86 $HV_{0.05}$ in the proximity of the coated layer (Fig. 11).

The laser cladding using a starter pre-placed paste lead to the formation of a glassy-ceramic coating on the surface of the copper plate, as it can be observed from both optical (Fig. 3 a) and SEM micrographs (Figs. 4 and 5).

The glassy-coating formation could be due to the synergistic action of three factors, namely: a) the high local temperatures reached through laser beam directional focusing on the surface of the sample; b) the high temperature gradients arising from the rapid cooling of the oxidic-HA melt and c) the presence of HA as glass forming agent, which impedes the crystallization of the oxides as ceramic.

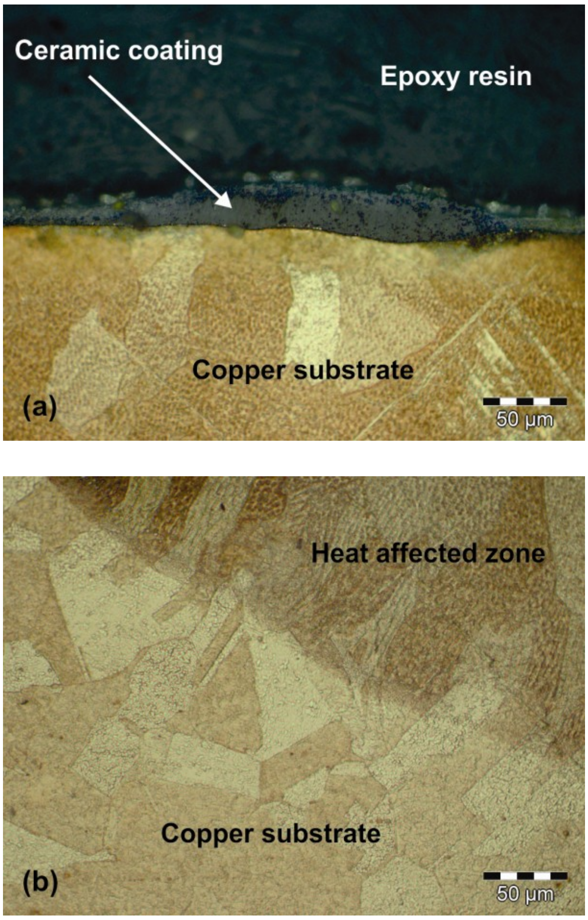

Fig. 3. (a) Optical microscopy of the ceramic coated layer and (b) the heat affected zone

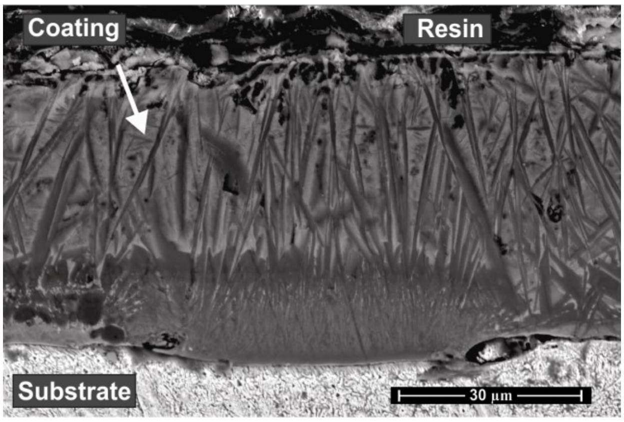

Fig. 4. SEM image of the ceramic coated layer

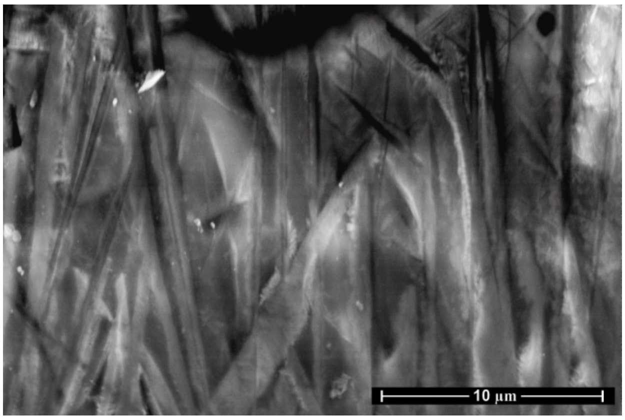

Fig. 5. Detail of the ($(Al_2O_3+TiO_2)/Al/HA$) amorphous coating fabricated by laser cladding

SEM microscopy from Fig. 5 reveals further insight on the microstructure of the obtained coating. As the oxidic-HA melt in contact with the base material (as copper can uniformly distribute and radiate heat) cools at a lower rate than the melt from the top of the material, in contact with the atmosphere, the bottom part of the coating is richer in crystalline ceramic phases entrapped in a dominatingly amorphous glassy matrix, while in the upper part, the glass phase is predominant. Throughout the glass phase, several columnar-shaped crystalline phases could be observed, almost perpendicular to the surface of the base material.

The dominatingly amorphous (glass) phase presence in the coating is also confirmed by XRD diffractogram data from Fig. 6 (the broad reflection peak from ~ 20.15°; 23.84° and 25.18°). The overall crystallinity of the coating, calculated as the sum of the peak areas of the crystalline phases, reported to the overall area under the diffractogram is 47.83%.

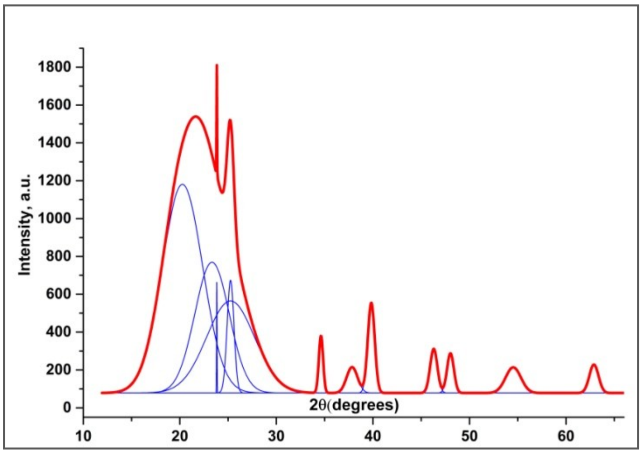

Fig. 6. XRD diffractogram of the obtained coating

From the diffractogram, the presence of several crystalline phases could be noted, coming from both compounds found in the original ceramic-starter powder, such as hydroxyapatite Ca_{10} (PO4)$_6$(OH)$_2$ (23.87°; 39.86°); α-Al_2O_3 (34,78°); TiO_2-rutile (54,57°), intermediary hydroxyapatite decomposition, such as β-$Ca_3(PO_4)_2$ (25.17°) or copper oxidation (CuO, at ~37.83°) products as well as new phases, such as Al_2TiO_5 (46.27°) and $CaTiO_3$ (~62.86°). These new phases could be embedded in both crystalline form in the glass-matrix, or they could form glass on their own, with the HA, decomposed HA-resulted TiO_2 and Al_2O_3 components.

Due to the presence of several reflections of the amorphous phases, it could be suggested that the glass matrix could be multiphasic, determined by the different diffusional processes of the glass-forming compounds in the laser-generated melt.

The role of HA could be therefore concluded as hard-phases generator (through forming IR-absorptive ceramic titanates) and as glass forming agent, either as calcium triphosphate, or mixed with Al and Ti oxides.

- Glass/ceramic forming compounds

$Ca_{10}(PO_4)_6(OH)_2 \rightarrow 2\ Ca_3(PO_4)_2 + Ca_4O(PO_4)_2 + H_2O$

- Ceramic forming compound

$Ca_4O(PO_4)_2 + TiO_2 \rightarrow CaTiO_3 + Ca_3(PO_4)_2$

- Mixed Al/Ti oxides (glass/ceramic forming)

$Al_2O_3 + TiO_2 \rightarrow Al_2TiO_5$

Our approach through determining a combined embedding and/or formation of IR-absorptive components into a glassy matrix protects the assembly from degradative factors, as well as ensuring a mechanical-resistant coating.

Our method eliminates the disadvantages of the traditional solar collectors obtaining, related to low economic efficiency (sequential processing) or environmental risks (potentially toxic precursors), through using an integrated laser-processing approach.

Also, by using glass in molten state, a more efficient covering of the substrate metal could be achieved than in the case of traditional spray pyrolysis techniques, due to the good wetting properties of molten glass. The presence of CuO, as depicted also from the XRD diffractogram could act as a compatibilizer between the base metal and the coating.

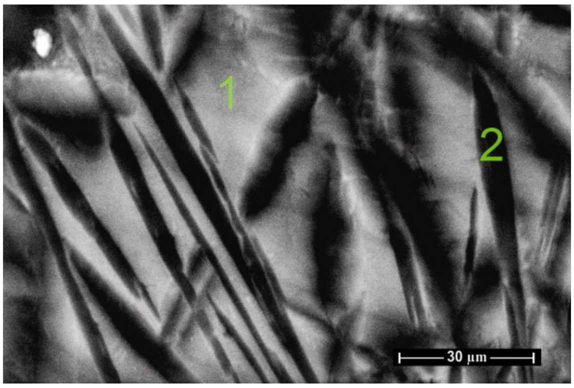

Fig. 7. Localization of the EDS spectrum realised on the glassy coating, white area, and dark area

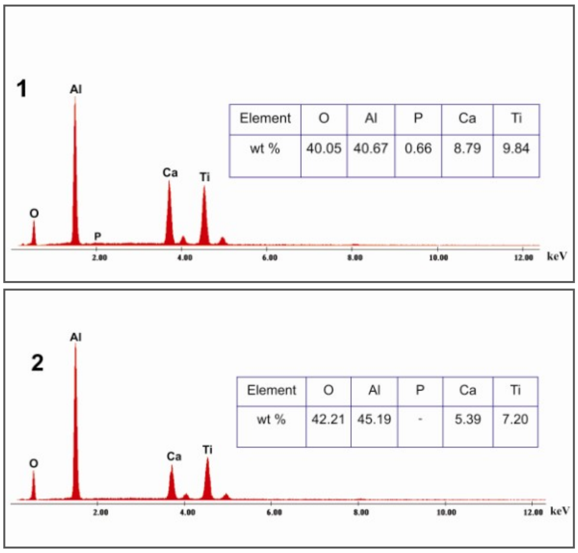

Element	O	Al	P	Ca	Ti
wt %	40.05	40.67	0.66	8.79	9.84

Element	O	Al	P	Ca	Ti
wt %	42.21	45.19	-	5.39	7.20

Fig. 8. EDX spectrum of the white (1) and black (2) area indicated in Fig. 6 (EDS set-up: kV: 30.00, Tilt: 0.10 Take-off: 5.45, AmpT: 12.80)

EDX spectrum (Fig. 8) on the glassy region of the coating reveals the presence of all the initial components from the powder mixture used for laser cladding (zone 1 from Fig. 7). The darker crystalline areas depicted in Fig. 7 (zone 2) contain a higher amount of aluminium, while containing no phosphorus.

They could be formed by large oxides/mixed oxides crystallites, which play an important role in tuning the optical properties of the assembly, as well as in contributing to the hardness (Fig. 11) and mechanical stability to the assembly.

From the cross-sectional EDX elemental distribution illustrated in Fig. 9 it could be observed that the surface of the coating is richer in Ca, Al, O and P, which are efficient glass-forming elements, while the coating in proximity to the base material is richer in Ti, a crystalline ceramic-forming element.

As it could be seen from Fig. 10 a, the obtained coating presents good transparency in the 550-800 nm domain, reflecting the wavelengths corresponding to the copper substrate. This is particularly important in the field of designing non-black solar absorbent materials.

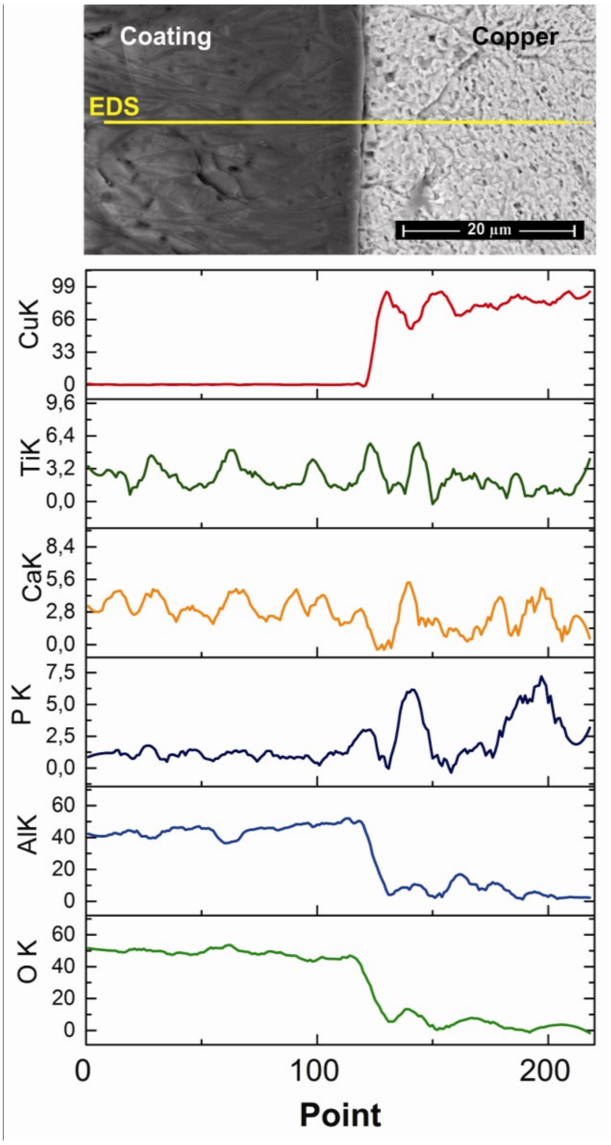

Fig. 9. EDS line spectrum analyze in the cross section of the specimen (Kv 20.0, Mag 7000, Tilt 0.0 Averaging 16)

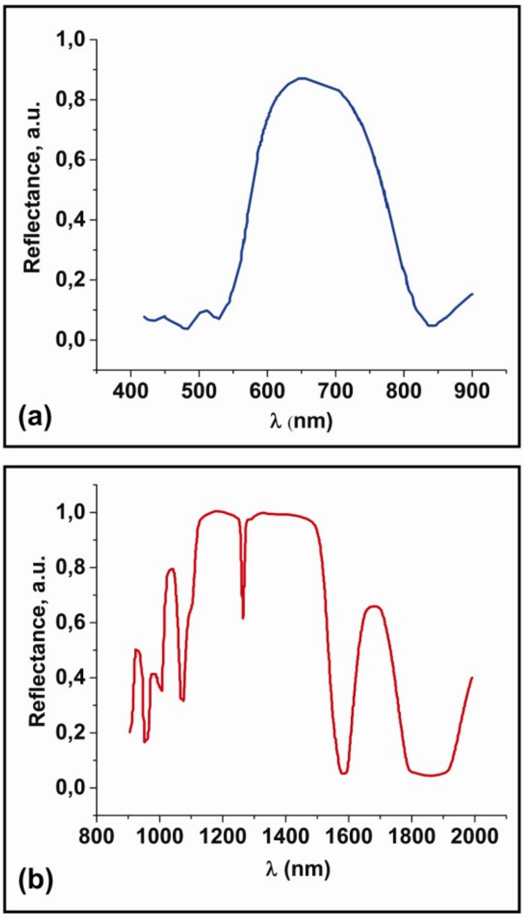

Fig.10. (a) VIS and (b) NIR reflectance spectra of the ceramic coating

The NIR spectra of the coating presents several absorption bands, such as those centered at ~1262 nm ascribed to -OH groups overtones (from HA or hydrated ceramic compounds); ~1862 nm, ascribed to P-O groups vibration overtones; ~1585 nm, ascribed to Ti-O vibration modes in TiO_2 and/or TiO_3^{2-} and 949 and 1075 nm, ascribed to Al-O bonds from Al_2O_3 and/or aluminates.

The solar absorptance (αs) of the material, theoretically defined as weighted fraction between absorbed radiation and incoming solar radiation in the wavelength interval 0.4– 2 µm, has been determined using equation 1[16].

$$\alpha_s = \frac{\int_{0.4}^{2} I_s(\lambda)(1-R(\lambda))d\lambda}{\int_{0.4}^{2} I_s(\lambda)d\lambda} \qquad (1)$$

where $I_s(\lambda)$ represents the solar spectra irradiance for a given mass of air, according to the ISO standard 9845-1 (1992) and $R(\lambda)$ represents the reflectance of the coating in the specified wavelength interval.

The value of the solar absorptance of the glass-ceramic coating obtained by our laser cladding method on copper substrate is α_s=0.816, comparable to other Al_2O_3 or Al_2O_3-MO_x systems (where MO= NiO, TiO_2, WO_3 and so forth) which fell in the range of 0.7-0.9.

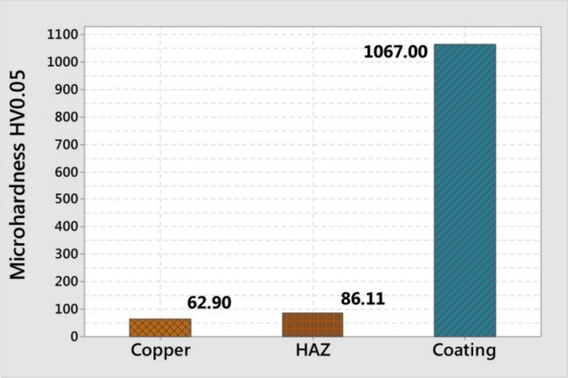

Fig. 11. Microhardness of ceramic coating, copper substrate and heat affected zone

The average hardness value of the coating is up to 16 times higher than that of the substrate, proving the formation of hard glassy/ceramic phases, but also with brittleness low enough to prevent the cracking of the sample during analysis.

Further studies are needed to improve the bonding with the substrate and to characterize the thermal emittance of the glassy-ceramic coating, as well as its stability to degradative factors (metal ions leaching from the glass matrix, wear resistance). Also, by tuning the operational parameters such as the ratio between the components from the glass/ceramic starter powder and the laser cladding regime, materials with improved optical properties (high absorptance and low thermal emittance coefficients) can be obtained using this method.

4. Conclusions

In this paper, a glass/ceramic Al_2O_3-TiO_2 composite coating has been obtained through laser cladding directly on the copper substrate, without the addition of a buffer layer. The addition of hydroxyapatite in the composition of the glass/ceramic starter lead to the obtaining of a crack-free glassy matrix, in which several titanate/aluminate columnar-shaped hard crystalline phases could be observed, almost perpendicular to the surface of the base material. The glassy/ceramic coating presents high hardness values.

The assembly presents promising potential as use in non-black solar-collectors designing. The solar absorptance coefficient of the coating is 0.816, comparable with other Al_2O_3-based materials, and the transparency of the coating is optimal in the 500-800 nm domain.

By using the laser cladding approach presented in this paper, novel IR-absorptive coatings could be designed in a one-step procedure, eliminating traditional sequential processing (deposition of powders starting from precursors, annealing and so forth) while being more environmental friendly. The high price of the laser treatment method could be overcome by the obtaining of efficient, corrosion-resistant coatings. Further studies are needed to assess the chemical and environmental stability of the obtained coating, as well as for fine tuning the composition of the ceramic starter, to obtain materials compatible to a sustainable development of the society.

References

[1] R. J. Lawrence, D. Waugh, Laser Surface Engineering: Processes and Applications, Woodhead Publishing, (2015).

[2] A. Pascu, Parameters of the laser cladding process, Luxlibris Publishing, (2015).

[3] G. Popescu-Pelina, F. Sima, L. E. Sima, C. N. Mihailescu C. Luculescu, I. Iordache, M. Socol, G. Socol, I. N. Mihailescu, Applied Surface Science, oct. 2016.

[4] H. Nishikawa, T. Hasegawa, A. Miyake, Y. Tashiro, Y. Hashimoto, D. H.A. Blank, G. Rijnders, Materials Letters **165**, 95 (2016).

[5] B. R. Gligorijević, M.b Vilotijevićb, M. Šćepanović, D. Vidović, N. A. Radović, Journal of Alloys and Compounds **687**, 421 (2016).

[6] R. I. M. Asri, W. S. W. Harun, M. A. Hassan, S. A. C. Ghani, Z. Buyong, Journal of the Mechanical Behavior of Biomedical Materials **57**, 95 (2016).

[7] B. A. Sava, C. Tardei, C. M. Simonescu, L. Boroica, A. Melinescu, Optoelectron. Adv. Mat. **9**, 1415 (2015).

[8] C. Paraschiv, I. Stirbu, R. Cimpoesu, M. Bernevig, C. Nejneru, V. Manole, N. Cimpoesu, G. Zegan, Optoelectron. Adv. Mat. **10**, 87 (2016).

[9] G. Armencea, C. Berce, H. Rotaru, S. Bran, V. Stefan, D. Leordean, C. -A. Jula, D. Gheban, M. Lazar, G. Baciut, M. Baciut, R. S. Campian, Optoelectron. Adv. Mat. **9**, 865 (2015).

[10] D. G.Wang, C. Z. Chen, J. Ma, G. Zhang, Colloids and Surfaces B: Biointerfaces **66,** 155 (2008).

[11] X. Pei, J. Wang, Q. Wan, L. Kang, M. Xiao, H. Bao, Surface & Coatings Technology **205,** 4380 (2011).

[12] C. S. Chien, T. F. Hong, T. J. Han, T. Y. Kuo, T. Y. Liao, Applied Surface Science **257,** 2387 (2011).

[13] Y. Chen, D. Wu, G. Ma, W. Lu, D. Guo, Surface & Coatings Technology **228,** 452 (2013).

[14] G. Xue-song, T. Zong-jun, L. Zhi-dong, S. Li-da, Trans. Nonferrous Met. Soc. China **22**, 2498 (2012).

[15] A. Berni, M. Mennig, H. Schmidt, Sol-Gel Technologies for Glass Producers and Users, Springer US (2004), p. 88, 2004.

[16] A. Duta, L. Isac, A. Milea, E. Ienei, D. Perniu, Energy Procedia **48,** 543 (2014).

---

*Corresponding author: alexandru.pascu@unitbv.ro;
pascu.alex@yahoo.com